A coherent image source method for flat waveguides with locally reacting boundaries

Hequn Min, Xiaojun Qiu and Ningrong Li

Key Laboratory of Modern Acoustics and Institute of Acoustics, Nanjing University, Nanjing, CHINA
Email address: hqmin@nju.edu.cn (Hequn Min)

PACS: 43.55.Ka, 43.55.Br

ABSTRACT

An image source method is presented for coherently evaluating the sound field from a point source in flat waveguides with two infinite and parallel locally reacting boundaries, where one is sound absorbing and the other is reflective. The method starts from formulating sound reflections into integrals by plane wave expansion, and the inherent intractability in solving these integrals in such spaces is avoided by introducing a physically plausible assumption that wave fronts remain the same before and after the reflection on a near-rigid boundary. By comparisons to the classical wave theory and the existing coherent ray-based methods, it is shown that the proposed method is considerably accurate to predict the sound propagation in flat waveguides with a sound absorbing ceiling and a reflective floor over a broad frequency range and for various source/receiver geometries, even if at large distances from the source compared to the waveguide height while the existing methods are shown to be erroneous.

INTRODUCTION

Speech privacy and noise control problems are often encountered in open-plan offices and appear serious in large ones [1]. These rooms usually have heights much smaller than the lateral dimensions, reflective floors, and suspended ceilings lined with sound absorbing material. A simplified model for such rooms can be a flat waveguide with two infinite parallel boundaries (floor and ceiling) with locally reactive material.

There have been many methods for predicting the sound field inside a flat waveguide. Based on the incoherent image source method, Kuttruff [2] proposed analytical formulas to predict the sound energy distribution in flat waveguides in 1980s. With similar incoherent ray-based methods, many other researchers have studied sound fields in similar spaces, such as large fitted factories [3-6], workshops [7,8], and dinning rooms [9]. These models neglected the interference effect among direct sound and multiple reflections, and in some applications such as that for predicting sound fields of speech or narrow band noise, the models appear erroneous and cannot provide meaningful prediction [10-12].

There are some studies on the coherent ray-based method for the sound field in bounded spaces. Dance *et al.* [10] have developed an interference model to predict the sound pressure in industrial enclosures by considering the sound propagating phase shift and coherent summation of different reflected waves. Wang *et al.* [13] employed the image source method to coherently calculate the total field from a point source in open-plan offices by using the plane wave reflec-

tion coefficients for the reflections of spherical sound radiation of the image sources. Brekhovskikh [14] described the sound field in a flat-layered homogeneous media as sum of direct sound and multiple reflections from image sources, where each reflection is formulated as a form of plane wave expansion integral. In light of Brekhovskikh's work and based on the solution for the spherical wave reflection on an infinite plane, Gensane and Santon [15] proposed a generalized solution to effectively model the successive reflections of spherical sound radiation from a point source in bounded spaces having more than two planes. According to the concepts of Gensane and Santon, Lemire and Nicolas [11] replaced the reflection coefficient with a more accurate solution [16] of the spherical wave reflection on one infinite plane to numerically investigate the sound field in flat waveguides. Westwood [17] has proposed a ray-based method for sound fields in flat waveguides with a penetrable bottom boundary and an idealized sound-soft top boundary to model the shallow water ocean environment.

However these previous coherent ray-based methods either require spaces bounded with sufficiently hard boundaries at high frequencies, or appear erroneous when source/receiver distance being large compared to the height in the flat waveguide with a sound absorbing ceiling and a reflective floor, which is a common situation in large fitted open-plan offices. In this paper, research is presented toward a simple but accurate coherent model to predict the sound propagation in flat waveguides with a sound absorbing ceiling and a reflective floor, particularly at large distances from the source compared to the space height.

THEORETICAL METHOD

Formulation of the problem

Figure 1(a) shows a vertical section of a flat waveguide, where the ceiling and floor are locally reactive with uniform normalized specific admittance of β_c and β_f respectively. The height of the space is h, a point source is at $(0, z_s)$ and a receiver is at (r, z) with r being the horizontal distance from the source to receiver. The time-dependant factor $e^{-j\omega t}$ is suppressed for simplicity throughout this paper.

(a)

(b)
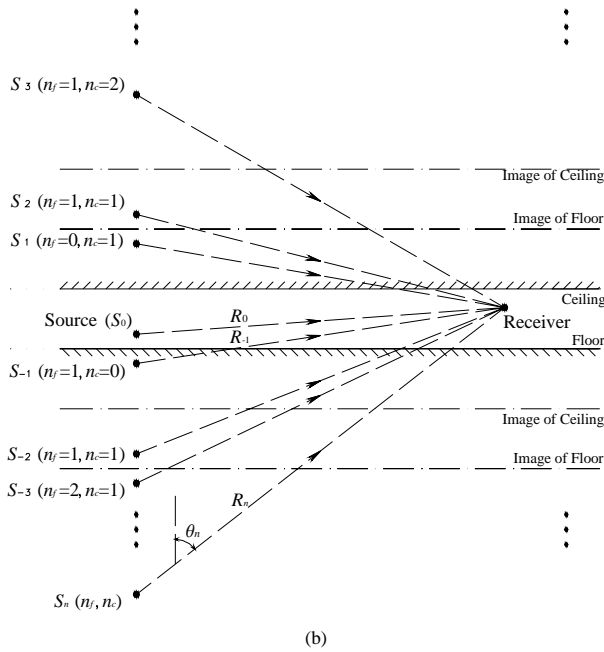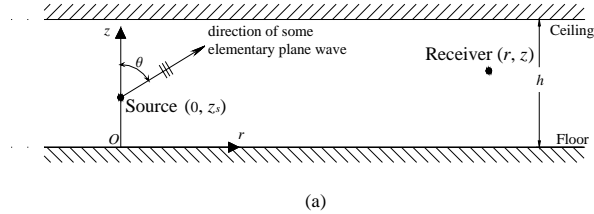
Figure 1. Vertical section of a typical flat waveguide. (a) The source and receiver geometry. (b) The schematic geometry of image sources, where the real source is assumed to be S_0, R_n denote the propagation distances of the corresponding ray from the nth image source to the receiver and θ_n represents the incident angle of each ray to the horizontal boundaries.

Based on the plane wave expansion of the spherical wave, the Green function in free field can be expressed as [14]

$$\frac{e^{jkR_0}}{4\pi R_0} = \frac{jk}{8\pi^2} \int_0^{2\pi} \int_0^{\frac{\pi}{2}-j\infty} e^{j\vec{k}\cdot\vec{R}_0} \sin\theta \, d\theta \, d\varphi \,, \qquad (1)$$

where $\vec{k} = k(\sin\theta\cos\varphi, \sin\theta\sin\varphi, \cos\theta)$ and k is the wave number. $\vec{R}_0$ is the distance vector from the source to the receiver with quantity of R_0. θ and φ represent the azimuth angles in cylindrical coordinates characterizing the direction of each plane wave propagation in vertical and horizontal planes respectively.

In the absence of the ceiling, the reflection of spherical wave incidence can be obtained by the superposition of all the elementary plane wave reflections on the floor plane as [14]

$$P_{-1} = \frac{jk}{8\pi^2} \int_0^{2\pi} \int_0^{\frac{\pi}{2}-j\infty} e^{j\vec{k}\cdot\vec{R}_{-1}} V_f(\theta)\sin\theta \, d\theta \, d\varphi \,, \qquad (2)$$

where P_{-1} denotes the field of the first reflection on the floor plane shown in Fig. 1(b), and $\vec{R}_{-1}$ is the corresponding distance vector from the image source S_{-1} to the receiver. $V_f(\theta)$ represents the plane wave reflection coefficient of the floor at incidence angle θ and is given by

$$V_f(\theta) = \frac{\cos\theta - \beta_f}{\cos\theta + \beta_f} \,. \qquad (3)$$

With the ceiling, the total field can be constructed with the rays from an infinite number of image sources [14] with an expression of

$$P_{tot} = \sum_{n=-\infty}^{+\infty} P_n \,, \qquad (4)$$

in which $n = 0, \pm1, \pm2, \ldots$, and P_n represents the ray contribution from the nth image source shown in Fig. 1(b). Particularly P_0 denotes direct sound from the real source. Similar to Eq. (2), the ray contribution from the path with n_f floor reflections and n_c ceiling reflections can be expressed with an integral [14]

$$P_n = \frac{jk}{8\pi^2} \int_0^{2\pi} \int_0^{\frac{\pi}{2}-j\infty} e^{j\vec{k}\cdot\vec{R}_n} [V_f(\theta)]^{n_f} [V_c(\theta)]^{n_c} \sin\theta \, d\theta \, d\varphi \,, \qquad (5)$$

where $\vec{R}_n = (r\cos\varphi_n, r\sin\varphi_n, R_n\cos\theta_n)$ is the distance vector from the nth image source S_n to the receiver, θ_n and φ_n denote the azimuth angles to characterize the direction of $\vec{R}_n$ in vertical and horizontal planes respectively. $V_c(\theta)$ is the plane wave reflection coefficient on ceiling boundary and is expressed as

$$V_c(\theta) = \frac{\cos\theta - \beta_c}{\cos\theta + \beta_c} \,. \qquad (6)$$

The orders n_f and n_c can be determined from the order n with a rule of

$$n_f = \frac{|n|}{2} - \frac{1}{2}\mathrm{sign}(n)\mathrm{rem}(|n|,2) \,, \qquad (7a)$$

and

$$n_c = \frac{|n|}{2} + \frac{1}{2}\mathrm{sign}(n)\mathrm{rem}(|n|,2) \,, \qquad (7b)$$

where sign(.) denotes the signum function, and $\mathrm{rem}(|n|,2)$ represents the remainder of $|n|$ after division by 2.

Defining an overall coefficient $V(\theta)$ to replace the term $[V_f(\theta)]^{n_f} [V_c(\theta)]^{n_c}$, P_n in Eq. (5) is rewritten as

$$P_n = \frac{jk}{8\pi^2} \int_0^{2\pi} \int_0^{\frac{\pi}{2}-j\infty} e^{jk[r\sin\theta(\cos\varphi\cos\varphi_n+\sin\varphi\sin\varphi_n)+R_n\cos\theta\cos\theta_n]} V(\theta)\sin\theta \, d\theta \, d\varphi \,, \qquad (8)$$

and then can be further transformed into

$$P_n = \frac{jk}{8\pi^2} \int_0^{\frac{\pi}{2}-j\infty} \left\{ \int_0^{2\pi} e^{jkr\sin\theta\cos(\varphi-\varphi_n)} d\varphi \right\} e^{R_n\cos\theta\cos\theta_n} V(\theta)\sin\theta\, d\theta \,. \qquad (9)$$

By using [14,18]

$$\int_0^{2\pi} e^{jkr\sin\theta\cos(\varphi-\varphi_n)} d\varphi \equiv 2\pi J_0(kr\sin\theta) \,, \qquad (10)$$

where $J_0(.)$ represents the Bessel function of zero order, Eq. (9) can be simplified as

$$P_n = \frac{jk}{4\pi} \int_0^{\frac{\pi}{2}-j\infty} e^{jkR_n\cos\theta\cos\theta_n} V(\theta) J_0(kr\sin\theta)\sin\theta\, d\theta \,. \qquad (11)$$

Using the identities for a complex number u that $J_0(u) = \left[H_0^1(u) + H_0^2(u)\right]/2$ and $H_0^2(-u) = -H_0^1(u)$, Eq. (11) can be written as

$$P_n = \frac{jk}{8\pi} \int_{\frac{\pi}{2}+j\infty}^{\frac{\pi}{2}-j\infty} V(\theta)\sin\theta \cdot H_0^1(kr\sin\theta)\, e^{jkR_n\cos\theta\cos\theta_n} d\theta \,, \qquad (12)$$

in which $H_0^1(.)$ and $H_0^2(.)$ are the Hankel functions of first and second kind with zero order. Now the total field from a point source in a flat waveguide is explicitly formulated by Equation (4) accompanied with the integral Equation (12).

The coherent image source method

As shown in Fig. 1(b), P_0 is the direct sound $e^{jkR_0}/4\pi R_0$, and P_1 and P_{-1} is the field of single reflections whose integral expressions with Eq. (12) can be evaluated with the exact (integral) solution provided by Nobile *et al.* [19],

$$P_1 = \frac{e^{jkR_1}}{4\pi R_1}\left[1 - \frac{4jk\beta_c BR_1}{\beta_c + \cos\theta_1} I(k, R_1, \beta_c, \theta_1)\right], \qquad (13a)$$

$$P_{-1} = \frac{e^{jkR_{-1}}}{4\pi R_{-1}}\left[1 - \frac{4jk\beta_f BR_{-1}}{\beta_f + \cos\theta_{-1}} I(k, R_{-1}, \beta_f, \theta_{-1})\right], \qquad (13b)$$

where $I(.)$ is an integral function given by

$$I(k, R_n, \beta, \theta_n) = \int_0^{\infty} \frac{e^{-jkR_n(t^2+2Bt)}}{\sqrt{1 - t^2/H - 2Bt/H}} dt \,, \qquad (14)$$

and β is the normal specific admittance of the plane that the reflection takes place on.

$$B = -j\sqrt{1 + \beta\cos\theta_n - (1-\beta^2)^{1/2}\sin\theta_n} \,, \qquad (15a)$$

and

$$H = 1 + \beta\cos\theta_n + (1-\beta^2)^{1/2}\sin\theta_n \,. \qquad (15b)$$

For the ray with multiple reflections ($|n|\geq 2$) on boundaries, though the exact solution of integral expression of P_n in Eq. (12) is generally not possible, it is feasible to analytically approximate such integral with the method of steepest descents for larger kr [14,16]. A second order approximate solution provided by Brekhovskikh [14] in term of asymptotic series with accuracy to terms of $1/(kR_n)^2$ is

$$P_n = \frac{e^{jkR_n}}{4\pi R_n} V(\theta_n) - \frac{e^{jkR_n}}{4\pi R_n}\frac{j}{2kR_n}\left[V'(\theta_n)\cot\theta_n + V''(\theta_n)\right] + \dots, \qquad (16)$$

where $V'(\theta_n)$ and $V''(\theta_n)$ represent the first and second derivative of $V(\theta)$ at θ_n, and $V(\theta) = [V_f(\theta)]^{n_f}[V_c(\theta)]^{n_c}$. Although Eq. (16) can be used in flat waveguides directly, its convergence needs to be analyzed before the application in the circumstance concerned in this paper. After substituting the expressions of $V_f(\theta)$ and $V_c(\theta)$ in Eqs. (3) and (6) into Eq. (16), a common factor of $\left[(\cos\theta_n + \beta_f)^{n_f}(\cos\theta_n + \beta_c)^{n_c}\right]^{-1}$ can be found in all the series terms in Eq. (16).

In the current circumstance, the floor is sound reflective, which leads that $|\beta_f|\to 0$. If the receivers are far from the source compared to the waveguide height, which is a common situation in large open-plan offices, the incidence angle θ_n of rays at the first few orders will approach $\pi/2$ as shown in Fig. 1(b). This causes that $(\cos\theta_n + \beta_f)\to 0$ and then limits the convergence radius of the asymptotic series in Eq. (16). The second order approximation in Eq. (16) is not sufficiently accurate for the current problem theoretically.

To explicitly obtain the higher orders of the asymptotic series in Eq. (16), exponential complexity will be encountered as the order increases [14,15] and such extension appears not sensible as the common factor $\left[(\cos\theta_n + \beta_f)^{n_f}(\cos\theta_n + \beta_c)^{n_c}\right]^{-1} \to \infty$ [16]. The steepest descent method modified by subtraction of the pole has been employed to remedy the similarly worsen accuracy of the asymptotic series for sound propagation along a single reflective boundary [16,20]. The modified method is based on the Laurent series expansion of the integrand in Eq. (2) to avoid the singularities from the poles. Nonetheless such strategy becomes difficult in the cases of flat waveguides with two boundaries, because the poles in this case come from the denominator $(\cos\theta + \beta_f)^{n_f}(\cos\theta + \beta_c)^{n_c}$ of the integrand in Eq. (12) and mostly are high order ones. It is intractable to explicitly obtain the residues of this integrand at these higher poles for Laurent series expansion.

Analysis on the physics of the problem might be helpful to get over the mathematical intractability above. The solution in Eq. (13a) or (13b) for the singly reflected field from a point source on an infinite plane can be rewritten for generality with a form of image source method as

$$P_{sr} = P_{dis} \cdot Q_{sr} \,, \qquad (17)$$

where P_{sr} is the field of single reflection of spherical wave from a point source on an infinite plane and P_{dis} is the direct field at receiver from the image source due to the single reflection. Q_{sr} is the single reflection coefficient for spherical wave incidence, and can be determined from Eq. (13a) or (13b) by

$$Q_{sr} = 1 - \frac{4jk\beta BR_n}{\beta + \cos\theta_0} \cdot I(k, R_n, \beta, \theta_n) \,, \qquad (18)$$

where R_n is the propagation distance of the ray and interpretations of other parameters are in accord with those in Eqs. (13a), (13b), and (14).

It is revealed that the reflected wave of the spherical sound incidence from an image source remains almost spherical along a hard enough boundary [21,22]. Thus according to Eq.

(17), each reflection of a ray on a reflective boundary that is denoted by RB, regardless of the reflection being the first or the successive one in the ray propagation from the spherical radiation, can be heuristically approximated by

$$P_r \approx P_{rp} \cdot Q_{ref}(IS, R \mid RB), \qquad (19)$$

where P_r denotes the ray field at receiver after a reflection on RB, and P_{rp} represents the expected ray field at the receiver if the boundary RB is rigid, which is just the perfectly reflected field on this boundary. $Q_{ref}(IS, R \mid RB)$ is used to replace the single reflection coefficient Q_{sr} for reflections on the reflective boundary RB and corresponds to the ray from the image source IS to receiver R, which is determined by Eq. (18) also.

In the current circumstance, the floor boundary is reflective. Thus before and after each reflection on it, the wave fronts can be assumed to remain the same. The ray field alterations after each reflection can be quantified by a weighting factor $Q_{ref}(IS, R \mid FB)$ that depends on the floor boundary (FB) and the ray geometry according to Eq. (19). Thus in the propagation of a ray with reflection order n_f on the floor and n_c on the ceiling shown in Fig. 1(b), after each "transmission" through the floor or its images, the propagation field of the ray with reflection order n should be once weighted by the reflection coefficient $Q_{ref}(S_n, R \mid FB)$. Therefore after the ray field being weighted for n_f times due to "transmission" through the floor and its images in propagation, the field contribution of the ray, P_n, can be approximated as

$$P_n \approx [Q_{ref}(S_n, R \mid FB)]^{n_f} \frac{jk}{8\pi} \int_{\frac{\pi}{2}+j\infty}^{\frac{\pi}{2}-j\infty} [V_c(\theta)]^{n_c} \sin\theta \cdot H_0^1(kr\sin\theta) e^{jkR_n\cos\theta\cos\theta_n} d\theta,$$
$$(20)$$

where $Q_{ref}(S_n, R \mid FB)$ can be determined from Eq. (18). Compared to Eq. (12), the integral of P_n in Eq. (20) has been simplified, and now the integrand involves only the reflection coefficient on the ceiling.

The integral in Eq. (20) describes the field of the ray after n_c times reflections on the absorbent ceiling. This can be evaluated by the second order approximation in Eq. (16) with ensured accuracy because $|\beta_c|$ does not approach zero and for the asymptotic series there is no singularity similar to that from $(\cos\theta_n + \beta_f) \to 0$ as $\theta_n \to \pi/2$. So P_n can be further approximated for larger kr by

$$P_n \approx [Q_{ref}(S_n, R \mid FB)]^{n_f} \left\{ V_t(\theta_n \mid CB, n_c) - \frac{j[V_t'(\theta_n \mid CB, n_c)\cot\theta_n + V_t''(\theta_n \mid CB, n_c)]}{2kR_n} \right\} \frac{e^{jkR_n}}{4\pi R_n},$$
$$(21)$$

where $V_t(\theta \mid CB, n_c)$ represents a total plane wave reflection coefficient to take account of the successive n_c times plane wave reflections on the absorbent ceiling boundary (CB) at an incident angle θ, which equals $[V_c(\theta)]^{n_c}$ in this case. $V_t'(\theta_n \mid CB, n_c)$ and $V_t''(\theta_n \mid CB, n_c)$ are the first and second derivatives of $V_t(\theta \mid CB, n_c)$ at θ_n respectively. The factor $e^{jkR_n}/4\pi R_n$ is the direct sound field at the receiver from the nth image source, while the factors in front of it act like a combined coherent reflection coefficient to evaluate the overall influence from all the successive reflections during the ray propagation. Hence P_n can be expressed as

$$P_n = Q_n \frac{e^{jkR_n}}{4\pi R_n}, \qquad (22)$$

where Q_n denotes the combined reflection coefficient corresponding to the ray with reflection order n and

$$Q_n \approx [Q_{ref}(S_n, R \mid FB)]^{n_f} Q_{abs}(S_n, R \mid CB, n_c), \qquad (23)$$

in which $Q_{abs}(S_n, R \mid CB, n_c)$ represents a total reflection coefficient taking account of all the successive reflections on an absorbent boundary for a ray with spherical radiation, where n_c times successive reflections have taken place on the absorbent ceiling during the propagation of the ray from S_n to R. The coefficient $Q_{abs}(S_n, R \mid CB, n_c)$ can be approximated by

$$Q_{abs}(S_n, R \mid CB, n_c) = V_t(\theta_n \mid CB, n_c) - \frac{j[V_t'(\theta_n \mid CB, n_c)\cot\theta_n + V_t''(\theta_n \mid CB, n_c)]}{2kR_n},$$
$$(24)$$

and $V_t(\theta \mid CB, n_c) = [V_c(\theta)]^{n_c}$.

Eqs. (22) and (23) are the main contribution of this paper, which in company with Eq. (4) delivers a coherent image source method to approximately solve the total field from a point source in flat waveguides with a sound absorbing ceiling and a reflective floor. In the next section, numerical simulations will be carried out to validate the model and compare it to the existing coherent ray-based methods.

NUMERICAL RESULTS AND DISCUSSIONS

The wave theory [23,24] is used as a reference to validate the ray-based methods being used for predicting the sound fields in flat waveguides concerned in this paper. The equations in the wave theory to solve the sound field from a point source in flat waveguides are detailed in the Ref. 11, 15, 23, 24 and not presented here for brevity. In simulations, the eigenvalue equation in the wave theory becomes complex for absorbent boundaries with complex admittance and is solved numerically [23-25]. For the image source methods, the locations of image sources can be determined through Fig. 1(b). The maximum order l is determined when the accumulated total field amplitude differs less than 0.1% from that accumulated up to the order $l+10$.

The Delany and Bazley model [26] is employed to evaluate the boundary admittances in simulations, which are given by

$$\beta = [1 + 0.057(\rho_0 f / \sigma)^{-0.754} - j0.087(\rho_0 f / \sigma)^{-0.732}]^{-1}, \qquad (25)$$

where β is the normalized specific boundary admittance, $\rho_0 = 1.293$ kg·m^{-3} denotes the air density at the room temperature, and f is the actuating frequency of sound wave. Parameter σ is the flow resistivity of boundary material with a unit of cgs (1 cgs = 1 kPa·s·m^{-2}). Although the Delany and Bazley model is semi-empirical and sometimes may be far from ideal to represent the realistic circumstance in open-plan offices, it is used in this paper due to its simpleness.Fig. 2 shows the normal incident absorption coefficient of materials with flow resistivities used hereafter versus frequency.
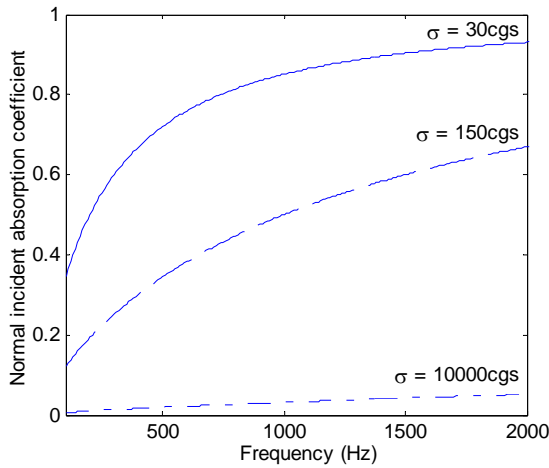
Figure 2. Spectra of normal incident absorption coefficient of materials with various flow resistivities σ in simulations.

Two numerical cases are investigated to access the prediction performance in flat waveguides by the proposed method and the existing coherent ray-based methods, such as the method of Brekhovskikh [14], the method of Lemire and Nicolas [11], and the method of Gensane and Santon [15]. The ceiling of the flat waveguide is assumed to be highly sound absorbing (30 cgs) in the first case and to be moderately absorbent (150 cgs) in the second, while the floor keeps reflective (10k cgs) and the waveguide height is always 2 m in both cases.

In the first case, the predictions of the sound pressure level (SPL) are firstly investigated versus r/h at 1000 Hz, where $z_s = z = 0.25$ m and the normal incident absorption coefficients of the ceiling and floor are 0.85 and 0.03 respectively. The corresponding results are compared in Fig. 3. It is shown that the results from the proposed method and those from the wave theory almost overlap over the range of r/h from 1 to 50. The method of Gensane and Santon [15] provides accurate results only when r/h is smaller than 2, and the method of Lemire and Nicolas [11] is accurate with r/h below 3. For the method of Brekhovskikh [14], large discrepancies are found between it and the wave theory as $r/h > 5$.
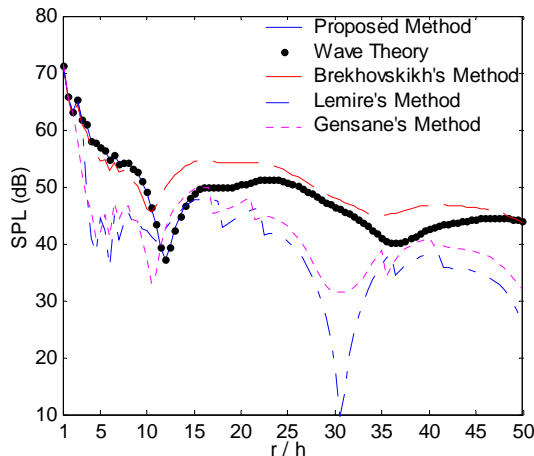
Figure 3. Predictions of SPL at frequency 1000 Hz versus r in a 2 m high flat waveguide. $z_s = z = 0.25$ m. The flow resistivities of the ceiling and floor are 30 and 10k cgs respectively.

Computations have been carried out in this case to further validate the proposed method in the frequencies range from 100 Hz to 2000 Hz, where receivers are chosen with a set of horizontal distances from the source of 5, 10, and 20 times of the waveguide height. Figures 4 shows the results corresponding to the situations where the source and receivers are at the height of a person seated ($z_s = z = 1.2$ m). The prediction of SPLs with the proposed method always agree well with the wave theory over a broad frequency range, except small differences observed at frequencies below 200 Hz, which may be explained by the reason that the accuracy of Eq. (16) is ensured in theory for large kr.
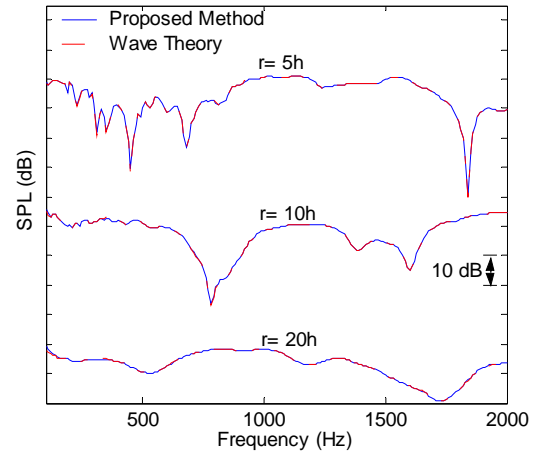
Figure 4. Spectra of SPL in the 2 m high flat waveguide investigated in Fig. 3, where $z_s = z = 1.2$ m.

In the second numerical case, the predicted SPL versus r/h curves with different methods are compared in Fig. 5, where $z_s = z = 0.25$ m and the frequency is 1000 Hz still for examination while the normal incident absorption coefficient of the ceiling becomes 0.5. The agreement between the proposed method and the wave theory is remarkable with r/h ranging from 1 to 50 again. The method of Brekhovskikh [14] is shown with errors also for r/h larger that 5 while the performance from the methods of Lemire et al. [11] and Gensane et al. [15] seem better by comparison with that in Fig. 4 of the first case, which might be explained by the less wave fronts distortion after each reflection on the ceiling as it being less absorbent. In this case, results similar to those in Fig. 4 in frequency domain were obtained by selecting the same source/receiver geometries, which are not presented here for brevity.
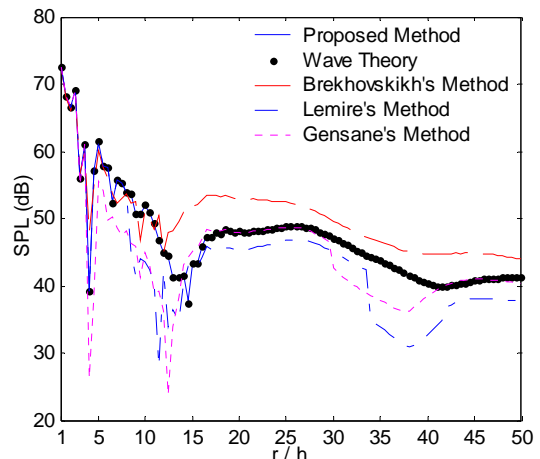
Figure 5. Same caption as Fig. 3 except that σ_c =150 cgs.

The computational time from the calculation with the proposed method and the numerical evaluation of the wave theory is also compared. In evaluation with the wave theory, the computational time increases exponentially with the frequency. At the highest frequency of 2000 Hz, it takes over 45 seconds for a personal computer with a 2.4 GHz Intel Q6600 processor to execute the numerical evaluation of the wave theory. However less one second is needed for the same computer to implement the calculation with the proposed method at a single frequency and the computational time is frequency independent. It is shown that the proposed method is simple and much faster than the numerical evaluation with the wave theory for an equivalent accuracy degree. From the above results for sound fields in the flat waveguide with a sound absorbing ceiling and a reflective floor, it is clear that the proposed coherent image source method is valid and can provide more accurate predictions than the existing coherent ray-based methods for various source/receiver geometries.

CONCLUSION

In the present study, an accurate coherent image source method has been derived to predict the sound fields in the flat waveguide with a sound absorbing ceiling and a reflective floor, which can be a simplified model for the fitted open-plan offices. Based on the theory of expending spherical wave into plane wave integrals, the method provides a physically meaningful prediction avoiding the intractability in analytically approximating the integrals in such flat waveguides, by introducing an assumption that wave fronts remain the same before and after each reflection on a reflective boundary. Numerical results compared to the wave theory and the existing ray-based coherent methods show that, the proposed method is valid and accurate to predict the sound propagation, even if at large distances from the source compared to the waveguide height while the existing coherent ray-based methods are inaccurate.

ACKNOWLEDGEMENTS

REFERENCES

1   M. Asselineau, "Noise control of laboratories: case studies," *Proc. Acoustics 08 Paris*, 5165-5169 (2008)

2   D. A. Bies and C. H. Hansen, *Engineering Noise Control Theory and Practice* (E & FN SPON, London & New York, 1996), 2nd ed.

3   E. A. Lindqvist, "Sound attenuation in larger factory spaces," *Acustica*. **50**, 313-328 (1982)

4   M. Hodgson, "On the prediction of sound fields in large empty rooms," *J. Acoust. Soc. Am.* **84,** 253-261 (1988)

5   M. Hodgson, "On the accuracy of models for predicting sound propagation in fitted rooms," *J. Acoust. Soc. Am.* **88,** 871-878 (1990)

6   S. M. Dance and B. M. Shield, "The complete image-source method for the prediction of sound distribution in non-diffuse enclosed spaces," *J. Sound Vib.* **201,** 473-489 (1997)

7   A. M. Ondet and J. L. Barbry, "Modeling of sound propagation in fitted workshops using ray tracing," *J. Acoust. Soc. Am.* **85,** 787-796 (1989)

8   M. Hodgson, "Ray-tracing evaluation of empirical models for predicting noise in industrial workshops," *Appl. Acoust.* **64**, 1033-1048 (2003)

9   J. Kang, "Numerical modeling of the speech intelligibility in dining spaces," *Appl. Acoust.* **63**, 1315-1333 (2002)

10   S. M. Dance, J. P. Roberts and B. M. Shield, "Computer prediction of sound distribution in enclosed spaces using an interference pressure model," *Appl. Acoust.* **44**, 53-65 (1995)

11   G. Lemire and J. Nicolas, "Aerial propagation of spherical sound waves in bounded spaces," *J. Acoust. Soc. Am.* **85,** 1845-1853 (1989)

12   R. Pirn, "Acoustical variables in open planning," *J. Acoust. Soc. Am.* **49**, 1340-1345 (1971)

13   C. Wang and J. S. Bradley, "A mathematical model for a single screen barrier in open-plan offices," *Appl. Acoust.* **63**, 849-866 (2002)

14   I. Brekhovskikh, *Waves in Layered Media* (Academic, New York, 1980), 2nd ed.

15   M. Gensane and F. Santon, "Prediction of sound fields in rooms of arbitrary shape: validity of the image sources method," *J. Sound Vib.* **63**, 97-108 (1979)

16   K. Attenborough, S. I. Hayek, and J. M. Lawther, "Propagation of sound above a porous half space," *J. Acoust. Soc. Am.* **68**, 1493-1501 (1980)

17   E. K. Westwood, "Ray methods for flat and sloping shallow-water waveguides," *J. Acoust. Soc. Am.* **85,** 1885-1894 (1989)

18   K. Liang, *Mathematical Methods of Physics* (Higher education Press, Beijing, 1998), 3rd ed. (In Chinese)

19   M. A. Nobile and S. I. Hayek, "Acoustic propagation over an impedance plane," *J. Acoust. Soc. Am.* **78,** 1325-1336 (1985)

20   C. F. Chien and W. W. Soroka, "Sound propagation along an impedance plane," *J. Sound Vib.* **43**, 9-20 (1975)

21   J. B. Allen and D. A. Berkley, "Image method for efficiently simulating small-room acoustics," *J. Acoust. Soc. Am.* **65,** 943-950 (1979)

22   U. Ingard, "On the reflection of a spherical sound wave from an infinite plane," *J. Acoust. Soc. Am.* **23,** 329-335 (1951)

23   H. Kuttruff, *Room Acoustics* (Applied Science, London, 1991), 3rd ed.

24   P. M. Morse and K. U. Ingard, *Theoretical Acoustics* (McGraw-Hill, New York, 1968)

25   Y. Long and H. Jiang, "Rigorous numerical solution to complex transcendental equations," *Int J. Infrared Milli.* **19**, 785-790 (1998)

26   M. E. Delany and E. N. Bazley, "Acoustical properties of fibrous absorbent materials," *Appl. Acoust.* **3**, 105-116 (1970)